Interaction and dephasing of center-of-mass quantized excitons in wide ZnSe/$Zn_{0.94}Mg_{0.06}Se$ quantum wells

H. P. Wagner,* A. Schätz, and R. Maier
Universität Regensburg, Institut Physik II, D-93040 Regensburg, Germany

W. Langbein and J. M. Hvam
Mikroelektronik Centret, The Technical University of Denmark, Building 345 e, 2800 Lyngby, Denmark
(Received 26 June 1997)

We investigate the interaction and dephasing of the excitons in wide ZnSe/$Zn_{0.94}Mg_{0.06}Se$ quantum wells by spectrally resolved, femtosecond four-wave mixing (FWM). Polarization-dependent measurements indicate that excitation-induced dephasing is the dominant FWM process. The biexcitons of the center-of-mass quantized heavy and light hole excitons are observed, showing binding energies of 3.5 meV. We determine the exciton scattering cross sections with incoherent and coherent excitons. The coherent cross section is found to be larger than the incoherent cross section, which is attributed to a stronger Pauli repulsion for coherent excitons. The exciton interaction rates with acoustic and optical phonons are deduced by their temperature dependencies. The acoustic-phonon scattering is found to be strongly reduced in the investigated wide wells due to the reduced accessible phonon wave vector. [S0163-1829(98)00803-0]

I. INTRODUCTION

Degenerate four-wave mixing (FWM) provides a powerful tool to study coherent electronic relaxation processes in bulk semiconductors and quantum-well (QW) structures. The physics underlying the FWM process is described in a simple way by the optical Bloch equations.[1,2] However, an explicit consideration of the Coulomb interaction and the fermionic nature of the electrons and holes necessitates the use of the semiconductor Bloch equations (SBE). The complexity of the SBE can be reduced using extended OBE's, modeling selected terms of the SBE, e.g., local-field effects (LFE),[3] excitation-induced dephasing (EID),[4–6] biexciton formation (BIF),[7,8] or similar exciton-exciton interactions.[9,10] These extended OBE reproduce most of the various observations in FWM, including quantum beat phenomena,[11–14] scattering processes of excitons with free carriers,[15–17] with excitons,[18–21] and with phonons.[22–24]

So far, these coherent phenomena have been mainly studied in high-quality III–V multi-QW structures.[3–18,22,23] Recently, major progress in the quality of wide-gap II-VI semiconductor structures has been made in search of blue-green semiconductor lasers.[25] Since wide-gap II-VI QW's possess a high exciton oscillator strength and a strong third-order nonlinearity,[26] they are well suited to study coherent transient phenomena by FWM.[19–21,27–32] Also, the high biexciton binding energy enables the spectral discrimination of the BIF contribution.[33,34]

In this paper, we report on subpicosecond FWM studies on center-of-mass (COM) quantized excitons in wide ZnSe/$Zn_{0.94}Mg_{0.06}Se$ single QW's (SQW's). The use of SQW's excludes propagation effects[35] and interference effects between QW's.[36] We observe pronounced quantum beats (QB's) between the different exciton states below the continuum. All excitons show a comparable dephasing time. BIF is observed for the lowest heavy-hole and light-hole excitons. We evaluate the contribution of the EID FWM process by polarization-dependent measurements. The exciton-exciton scattering rate is obtained by density-dependent experiments. The exciton interaction with acoustic and optical phonons is studied by temperature-dependent measurements, showing a strong optical-phonon interaction and the suppression of acoustic-phonon scattering.

II. SAMPLE CHARACTERIZATION AND EXPERIMENTAL DETAILS

The investigated ZnSe QW samples were grown pseudomorphically on (001) oriented GaAs by molecular-beam epitaxy.[37] The two-dimensional (2D) growth mode was monitored by *in situ* reflection high-energy electron diffraction (RHEED), which was also used to determine the growth rate via RHEED oscillations. The samples consist of a 16 nm- (20 nm) wide ZnSe single QW sandwiched between 23 nm-thick $Zn_{0.94}Mg_{0.06}Se$ barrier layers, respectively. The Mg content of the barriers was determined by x-ray diffraction. The samples are of high optical and structural quality, as was examined by transmission, photoluminescence (PL), photoreflection spectroscopy, by high-resolution (HR) transmission electron microscopy, and HR x-ray diffraction.[38]

Systematic PL studies on pseudomorphically grown $Zn_{1-x}Mg_xSe$/ZnSe SQW structures with different well widths and Mg contents yield a conduction-band offset parameter $Q_c = 0.13 \pm 0.1$,[39] where Q_c is defined as the ratio of the conduction-band offset to the total band offset in an unstrained situation. The strain shifts the band energies, leading to a strained Q_c of approximately 0.3, so that the ZnSe/$Zn_{0.94}Mg_{0.06}Se$ QW's show a type-I band alignment.

The PL spectra of the investigated 16- and 20 nm SQW's obtained at 2 K are given in Fig. 1. The barrier heavy-hole exciton X_h appears at an energy of 2.859 eV. The COM quantized ZnSe 1*s* heavy-hole excitons 11*h*, 12*h*, 13*h*, and the light-hole exciton 11*l* were identified by comparison with calculated exciton energies using the model of Mathieu,

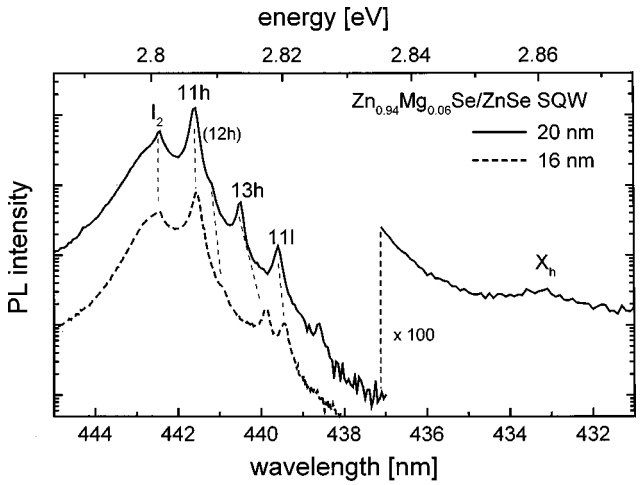

FIG. 1. PL spectra of the investigated 16- and 20-nm $Zn_{0.94}Mg_{0.06}Se/ZnSe$ SQW structures at excitation at 3.5 eV with 10 W/cm^2.

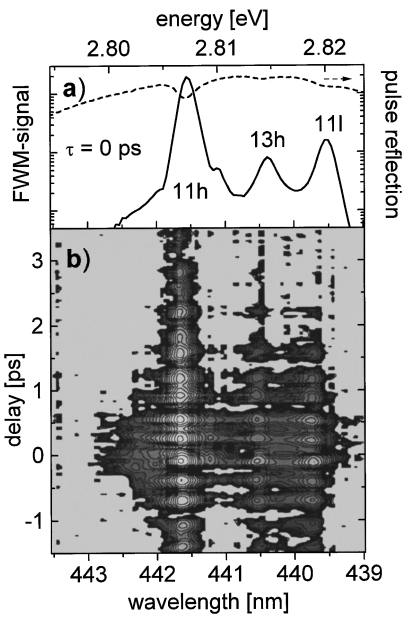

FIG. 2. FWM intensity from the 20-nm SQW in (↑↑) configuration. (a) FWM spectrum at zero delay and the spectrum of the reflected excitation pulse. (b) FWM intensity vs energy and delay time τ in a contour plot on a logarithmic scale over three decades.

Lefebvre and Christol.[40] The low-energy PL I_2 around 2.802 eV does not appear in photoreflection and absorption and is attributed to a donor bound exciton transition, presumably due to impurities from the Mg source. These assignments are supported by time-resolved PL experiments.

In the FWM experiments, the sample was excited by a frequency-doubled, mode-locked Ti-sapphire laser providing 100 fs pulses of 22 meV spectral width at a repetition rate of 76 MHz. The two-pulse degenerate FWM was performed in backscattering geometry, which is for SQW's as efficient as in transmission geometry. The focus diameter of the pulses at $1/e^2$ intensity on the sample was 70 μm. The FWM signal was detected time-integrated and spectrally resolved by a combination of a spectrometer and an optical multichannel analyzer as a function of the time delay τ between the two incident pulses. The sample was kept in a helium bath cryostat allowing for temperature-dependent measurements. If not otherwise mentioned, the experiments were carried out at a temperature of $T=5$ K.

III. FWM MECHANISMS

The FWM spectrum obtained from the 20 nm SQW at zero delay time is shown in Fig. 2(a) for colinear polarized (↑↑) excitation together with the spectrum of the reflected excitation pulse. The excitation energy was centered at 2.818 eV in order to avoid continuum contributions but simultaneously excite the 11h, 12h, 13h, and 11l states. The various exciton resonances are active both in reflection and FWM. In Fig. 2(b), the dependence of the FWM spectrum on the delay time is displayed. The FWM decay time of 0.7 ps is comparable for all excitonic resonances. Assuming a homogeneous broadening of the resonances, a dephasing time of $T_2=1.4$ ps is deduced. The corresponding homogeneous linewidth of 0.95 meV, given by $\Gamma_{\mathrm{hom}}=h/(\pi T_2)$, coincides with the spectral line width of 1.0 meV measured in the FWM spectra. The linewidth can thus be consistently explained by a homogeneous broadening mechanism. The simultaneous coherent excitation of the various exciton states leads to pronounced oscillations in delay time [Fig. 2(b)]. They are exactly in phase at all resonances, which is a signature of QB's.[2]

The different contributing FWM mechanisms can be discriminated by the FWM polarization dependence. The FWM trace at the 11h exciton is displayed in Fig. 3 for colinear (↑↑) and cross-linear (↑→) polarized excitation. At negative delay times, the conventional FWM process is inactive, and the observed FWM signal is caused by the LFE, EID, or BIF[3,5,7] In the LFE and EID cases, the first-order polarization enters twice into the signal generation process; therefore a decay twice as fast compared to positive delay

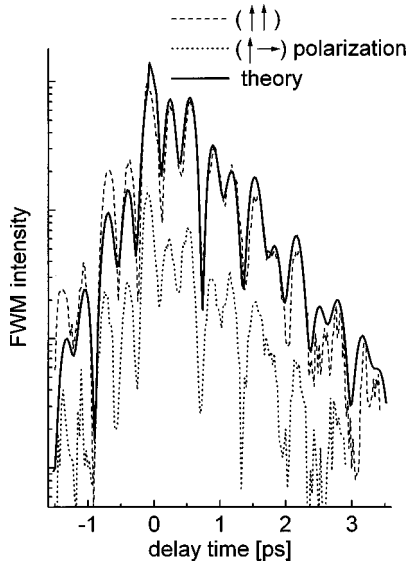

FIG. 3. FWM trace at the 11h exciton energy for (↑↑) (dashed line) and (↑→) (dotted line) configuration. The excitation was centered at 2.816 eV. The thick full line is a calculated trace based on a four-level OBE including EID using Eqs. (2) and (3).

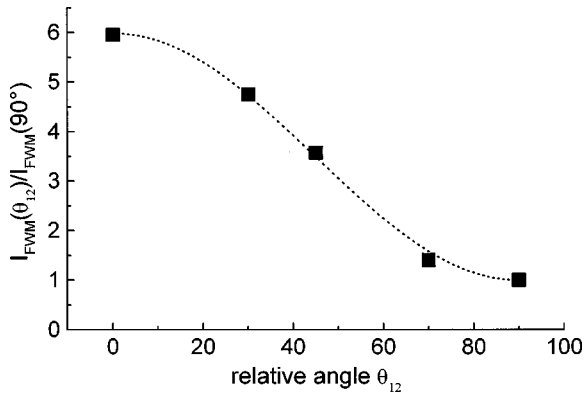

FIG. 4. Relative FWM intensity (squares) at the 11h exciton energy at $\tau=200$ fs as a function of the angle θ_{12} between the linear polarizations of the excitation pulses obtained from the 16 nm SQW. The dashed line is a fit using Eq. (1).

times is expected for negative delay times, as observed in the experiment. Since EID vanishes in the $(\uparrow\rightarrow)$ configuration, while LFE and BIF are not affected, the strong decrease of the FWM signal going from the $(\uparrow\uparrow)$ to the $(\uparrow\rightarrow)$ configuration shows that EID is the dominant FWM process in the $(\uparrow\uparrow)$ configuration. The dependence of the FWM intensity on the angle θ_{12} between the linear polarization directions of the excitation pulses is then expected to be[6]

$$I(\theta_{12})\propto\sin^2(\theta_{12})+\left[1+\frac{\sigma_{\mathrm{EID}}}{\gamma_2(n_X=0)}\right]^2\cos^2(\theta_{12}), \quad (1)$$

due to the variation of the spatial exciton density modulation. The relative FWM signal intensity $I(\theta_{12})/I(90°)$ observed at the 11h exciton from the 16 nm SQW at a delay time of 100 fs is shown in Fig. 4. A fit (dashed line) of Eq. (1) to the data using the determined values $\gamma_2(n_X=0)=0.7\ \mathrm{ps}^{-1}$ yields a EID cross section of $\sigma_{\mathrm{EID}}=97\times10^{10}\ \mathrm{s}^{-1}$. The dephasing time T_2 is not affected by the polarization configurations (see Fig. 3). This again confirms the dominant homogeneous broadening of the excitons, since in inhomogeneously broadened systems an increased dephasing with increasing angle θ_{12} is expected.[13] The observed predominant homogeneous broadening is attributed to the high-crystal quality and to the large width of the investigated QW structures leading to weak interface roughness and barrier alloy scattering.

The BIF contributes to the FWM signal for positive and negative delay time. It can be discriminated by the spectral splitting of a part of the signal by the biexciton binding energy below the exciton energy. Figure 5 shows the FWM spectra at $\tau=-0.8$ ps for $(\uparrow\uparrow)$, $(\uparrow\rightarrow)$ and cocircular $(\sigma^+\sigma^+)$ configuration, obtained at the 16 nm QW. The BIF-induced signal, denoted as XX, is equally strong in $(\uparrow\uparrow)$ and $(\uparrow\rightarrow)$ configuration, showing that the BIF process is not affected by EID, as expected in third-order perturbation theory.[7] It vanishes in the $(\sigma^+\sigma^+)$ configuration, since 11h biexcitons can only be formed with opposite spins. When 11h and 11l excitons are simultaneously excited biexcitons formed by both exciton species become visible in $(\uparrow\rightarrow)$ configuration as

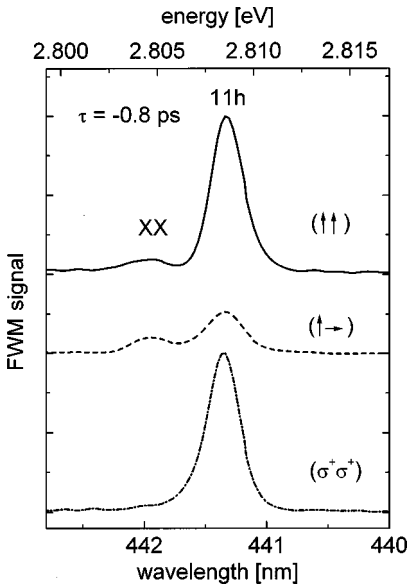

FIG. 5. FWM spectra from the 16-nm SQW at 0.8 ps negative delay in $(\uparrow\uparrow)$, $(\uparrow\rightarrow)$, and $(\sigma^+\sigma^+)$ configuration. The excitation was centered at 2.80 eV.

shown in Fig. 6 for the 20 nm SQW. The biexciton binding energies of the 11h and 11l biexcitons, denoted as $XX1$ and $XX2$ are determined to $E_{bXX}=3.5\pm0.5$ meV.

A more detailed analysis of the BIF signal and its relative importance to the FWM signal shows that the BIF FWM signal exceeds the LFE, but is weak compared to the EID contribution.[41] Accordingly, we modeled the FWM by the solution of optical Bloch equations for a homogeneously broadened four-level system similar to Ref. 2, that are extended only by EID.[5] The third-order response can be solved analytically in the perturbative regime, and the calculated Fourier transformed third-order polarization reads for positive delay,

$$P^{(3)}_{\mathrm{FWM}}(\omega,\tau>0)\propto\exp(i\omega\tau)\times\left(\sum_{i,j>1}^{4}\frac{2o_{ij}M_{i1}^2[M_{j1}^2\exp(i\Omega_{j1}^*\tau)]}{\omega-\Omega_{i1}}+i\sigma_{\mathrm{EID}}\sum_{i,j>1}^{4}\frac{o_{ij}M_{i1}^2[M_{j1}^2\exp(i\Omega_{j1}^*\tau)]}{(\omega-\Omega_{i1})^2}\right), \quad (2)$$

and for negative delay,

$$P^{(3)}_{\mathrm{FWM}}(\omega,\tau<0)\propto i\sigma_{\mathrm{EID}}\sum_{i,j>1}^{4}\frac{o_{ij}M_{i1}^2\exp(i\Omega_{i1}\tau)[M_{j1}^2\exp(i\Omega_{j1}\tau)]}{(\omega-\Omega_{i1})^2}. \quad (3)$$

The four considered levels i are the initially occupied ground state and the three excitons 11h, 11l, and 13h. The resonance energies ω_{i1} and dephasing rates γ_{i1} given by $\Omega_{i1}=\omega_{i1}-i\gamma_{i1}$ are determined from the FWM spectrum [Fig. 3(a)]. For simplicity, the dephasing rates $\gamma_{i1}=\gamma_{i1}(n_X=0)+\sigma n_X$ used in the EID process were taken to depend only on the total exciton density $n_X=(n_{21}+n_{31}+n_{41})$ of the

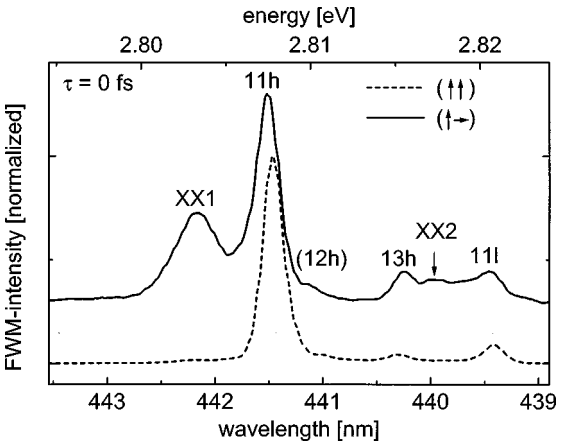

FIG. 6. FWM spectra from the 20-nm SQW at zero delay in the (↑→) and (↑↑) configuration. The excitation was centered between the 11*h* and 11*l* exciton energies at 2.815 eV. The biexcitonic transitions are labeled.

created 11*h*, 11*l*, and 13*h* excitons. The oscillator strength ratios $M_{21}^2:M_{31}^2:M_{41}^2$ were taken to 3:1:0.6 from the experimental reflection data. The EID parameter σ_{EID} was determined from the FWM intensity ratio between (↑↑) and (↑→) configuration. Furthermore, the spectral shape of the excitation was considered by the factors o_{ij} obtained from experimental data as described in Ref. 28. The calculated FWM trace at the 11*h* exciton, which is proportional to $|P_{\mathrm{FWM}}^{(3)}(\omega_{21},\tau)|^2$, is plotted in Fig. 3 (thick full line). It shows good agreement to the experimental data for positive delay, while for negative delay the signal is slightly underestimated due to the neglect of BIF and LFE.

IV. EXCITON-EXCITON SCATTERING

In order to investigate the exciton scattering rate with incoherent as well as with coherent excitons, density-dependent measurements were performed in the colinear polarization configuration. The excitation was tuned to mostly excite 11*h* excitons. For the scattering with incoherent excitons, a background density of 11*h* excitons is created by a prepump pulse applied 20 ps before the first FWM pulse. The FWM pulse intensities were kept constant and low compared to the prepump intensity. The scattering with mainly coherent excitons was studied in the two-beam configuration, changing the intensity of the excitation pulses equally. In this case, the character of the exciton-exciton scattering changes from coherent to incoherent with increasing delay time in the FWM experiment. The homogeneous line widths $\Gamma_{\mathrm{hom}}=h/(\pi T_2)$ obtained from the signal decay times are plotted in Fig. 7 as a function of the exciton density for both experimental situations. In both cases we find a linear increase of Γ_{hom} with increasing exciton density (Fig. 7), which is fit by

$$\Gamma_{\mathrm{hom}}(n_X)=\Gamma_{\mathrm{hom}}(n_X=0)+\gamma_X^{c,ic}n_X, \tag{4}$$

with the interaction parameter $\gamma_X^{c,ic}$ for the coherent and incoherent exciton-exciton scattering process, respectively. The 2D exciton density n_X created by the excitation pulses is estimated using the measured spot size, and the exciton absorption strength obtained from a free-standing $ZnSe/Zn_{0.94}Mg_{0.06}Se$ quantum-well structure that is adhesively bonded to a sapphire disk. The determined interaction parameters of $\gamma^{ic}=(2\pm0.6)\times10^{-11}$ meV cm^2 and $\gamma_X^c=(7\pm2)\times10^{-11}$ meV cm^2 differ significantly. Theories treating the coherent scattering process in closed form are not available so far. The higher value of the coherent scattering parameter compared to the incoherent scattering is, however, qualitatively explained by the increased repulsive interaction by Pauli exclusion, since the coherent excitons are concentrated in a smaller k space compared to the nearly thermalized incoherent excitons.

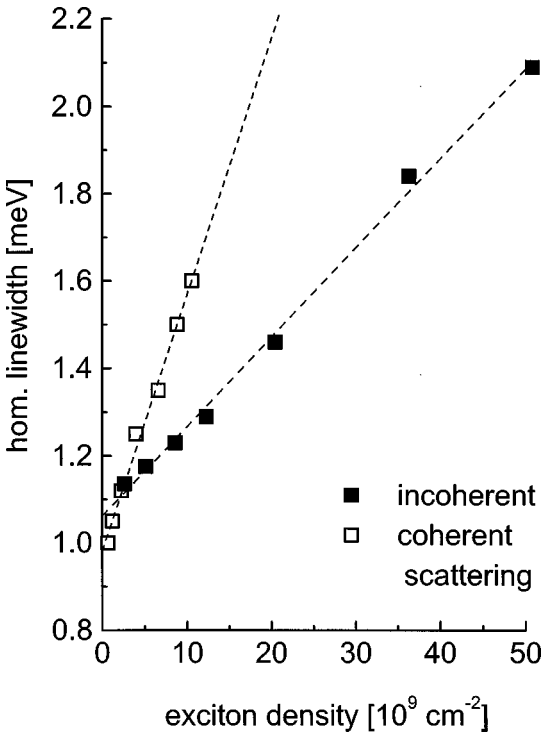

FIG. 7. Homogeneous linewidth corresponding to the measured dephasing times as a function of the exciton density for incoherent and mainly coherent scattering conditions for the 16-nm SQW. The dashed curves are fits according to Eq. (4).

The low-density and low-temperature homogeneous line width $\Gamma_{\mathrm{hom}}(n_X=0)$ is about 1 meV, and is attributed partly to the extrinsic interactions of excitons with donor impurities in the well. Recent FWM measurements on similar QW structures also indicate the presence of free electrons in the well originating from barrier impurities (donors). These free electrons lead to an intensity-independent electron-exciton scattering rate, which contributes to the background homogeneous linewidth.[41] Additionally, the radiative damping, which can be estimated to about 3 ps,[42] adds to the dephasing.

With an exciton binding energy of $E_{bX}\approx22$ meV and an exciton Bohr radius of $a_X\approx4.3$ nm, obtained from Ref. 40, a dimensionless parameter $\beta_X^{(2\mathrm{D})}=\gamma_X^{(2\mathrm{D})}/(a_x^2\times E_{bX})$ can be defined that is often used in experiments. In deriving E_{bX} and a_X the electron mass of $m_e^*=0.145m_0$ (Ref. 43) and the Luttinger parameters $\gamma_1=2.45$ and $\gamma_2=0.61$ (Ref. 44) are used. We find a value of $\beta_{Xic}^{(2\mathrm{D})}=4.7\pm1.4$ for the incoherent exciton-exciton scattering process, which is comparable to the result of previous investigations on $ZnS_xSe_{1-x}/ZnSe$ QW structures[32] and about twice the value found in GaAs QW's.[15,22]

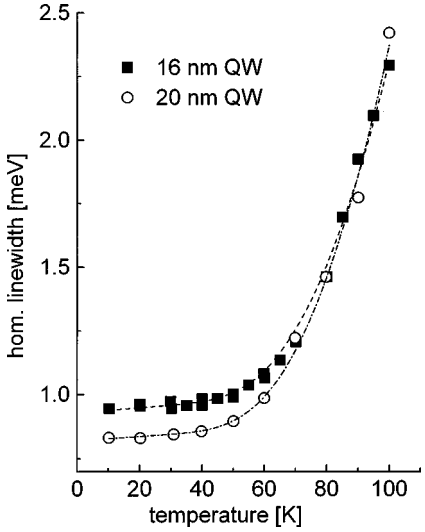

FIG. 8. Homogeneous linewidth corresponding to the measured dephasing times as a function of the lattice temperature for the 16- and 20-nm SQW. The dashed curves are fits according to Eq. (5).

V. EXCITON-PHONON SCATTERING

The influence of acoustic- and optical-phonon scattering on the exciton dephasing was measured by the temperature dependence of the dephasing time. Figure 8 shows the experimentally observed homogeneous linewidth as a function of the lattice temperature T for the 16 nm and the 20 nm SQW structure at low excitation densities ($n_X \approx 1 \times 10^9$ cm^{-2}). The temperature dependence of the decay rate exhibits two different regimes. Below 40 K, the decay rates are increasing weakly with temperature T due to acoustic-phonon scattering. At higher temperatures, a strong increase of the decay rate is observed, indicating the onset of optical-phonon scattering. The acoustic-phonon scattering parameter $\beta_{\rm ac}$ and the optical-phonon scattering parameter $\beta_{\rm LO}$ are fitted to the data according to the relation[45]

$$\Gamma_{\rm hom}(T,n_X)=\Gamma_{\rm hom}(T=0\ \ {\rm K},n_X)+\beta_{\rm ac}T + \frac{\beta_{\rm LO}}{\exp(E_{\rm LO}/k_BT)-1}, \qquad (5)$$

obtained by first-order perturbation theory. Here, $E_{\rm LO}=31.6$ meV is the longitudinal-optical phonon energy, k_B is the Boltzmann constant, and $\Gamma_{\rm hom}(T=0\ {\rm K},n_X)$ is the low-temperature homogeneous linewidth of 0.95 meV. For the acoustic-phonon–exciton interaction we obtain a value of $\beta_{\rm ac}=1\pm1$ μeV/K. This scattering parameter is significantly smaller than for quasi-3D and quasi-2D ZnSe structures ($\beta_{\rm ac}\approx4$–10 μeV/K).[24,32] The weak acoustic-phonon interaction is attributed to the large well width, limiting the quasi-momentum of the scattering phonons. A scattering rate inversely proportional to the well width is expected for the intrasubband scattering. Additionally, the acoustic phonons in the thin sample structure (total thickness of 62 nm) may be also deviating from a 3D character, changing the phonon density of states and the interaction cross section by the phonon reflection at the sample surface.

The deduced interaction parameter with optical phonons $\beta_{\rm LO}=51\pm4$ meV is comparable to the value in ZnS_xSe_{1-x}/ZnSe QW structures,[32] and significantly exceeds the value obtained from GaAs QW's ($\beta_{\rm LO}\approx10$ meV) (Ref. 8) due to the higher polarity of the II-VI material compared to the III-V compounds.

IV. SUMMARY

We have performed transient FWM experiments to study the dephasing of homogeneously broadened COM excitons in wide ZnSe/$Zn_{0.96}Mg_{0.06}$Se SQW's. Pronounced quantum beats are observed between the various exciton resonances, which can be described by extended OBE's. They include EID, which is found to be the dominant FWM process. Biexcitons of the 11h and 11l excitons show a biexciton binding energy of $E_{bXX}=3.5\pm0.5$ meV. The exciton-exciton interaction between incoherent excitons is lower than between coherent excitons. This behavior may be attributed to a higher repulsing interaction due to the Pauli exclusion principle for coherent excitons.

The optical-phonon exciton scattering is found to be enhanced due to the strong Fröhlich interaction in the higher polar II-VI material. The determined acoustic-phonon exciton scattering is very weak, a consequence of the large well width.

ACKNOWLEDGMENTS

The experimental support of K. Litvinenko and V. Mizeikis and enlightening discussions with D. Birkedal are kindly acknowledged. We thank T. Reisinger and W. Gebhardt for providing the $Zn_{0.94}Mg_{0.06}$Se/ZnSe QW structures. This work was supported by the Deutsche Forschungsgemeinschaft and by the Danish Ministries of Research and Education in the framework of CNAST.

*Author to whom correspondence should be addressed. FAX:++49 9419434226. Electronic address: Hans-Peter.Wagner@physik.uni-regensburg.de

[1] T. Yajima and Y. Taira, J. Phys. Soc. Jpn. **47**, 1620 (1979).
[2] J. Erland and I. Balslev, Phys. Rev. A **48**, R1765 (1993).
[3] M. Wegener, D. S. Chemla, S. Schmitt-Rink, and W. Schäfer, Phys. Rev. A **42**, 5675 (1990).
[4] H. Wang, K. Ferrio, D. G. Steel, Y. Z. Hu, R. Binder, and S. W. Koch, Phys. Rev. Lett. **71**, 1261 (1993).
[5] H. Wang, K. B. Ferrio, D. G. Steel, P. R. Berman, Y. Z. Hu, R. Binder, and S. W. Koch, Phys. Rev. A **49**, R1551 (1994).
[6] Y. Z. Hu, R. Binder, S. W. Koch, S. T. Cundiff, H. Wang, and D. G. Steel, Phys. Rev. B **49**, 14 382 (1994).
[7] H. Wang, J. Shah, T. C. Damen, and L. N. Pfeiffer, Solid State Commun. **91**, 869 (1994).
[8] E. J. Mayer, G. O. Smith, V. Heuckeroth, J. Kuhl, K. Bott, A. Schulze, T. Mayer, D. Bennhardt, S. W. Koch, P. Thomas, B. Hey, and K. Ploog, Phys. Rev. B **50**, 14 730 (1994).
[9] K. Bott, O. Heller, D. Bennhardt, S. T. Cundiff, P. Thomas, E. J. Mayer, G. O. Smith, R. Eccleston, J. Kuhl, and K. Ploog, Phys. Rev. B **48**, 17 418 (1993).
[10] E. J. Mayer, G. O. Smith, V. Heuckeroth, J. Kuhl, K. Bott, A. Schulze, T. Meier, S. W. Koch, P. Thomas, R. Hey, and K. Ploog, Phys. Rev. B **51**, 10 909 (1995).
[11] E. O. Göbel, K. Leo, T. C. Damen, J. Shah, S. Schmitt-Rink, W.

Schäfer, J. F. Müller, and K. Köhler, Phys. Rev. Lett. **64**, 1801 (1990).
[12] K. Leo, T. C. Damen, J. Shah, and K. Köhler, Phys. Rev. B **42**, 11 359 (1990).
[13] D. Bennhardt, P. Thomas, R. Eccleston, K. J. Mayer, and J. Kuhl, Phys. Rev. B **47**, 13 485 (1993).
[14] J. Erland, D. Birkedal, V. G. Lyssenko, and J. M. Hvam, J. Opt. Soc. Am. B **13**, 981 (1996).
[15] L. Schultheis, J. Kuhl, A. Honold, and C. W. Tu, Phys. Rev. Lett. **57**, 1635 (1986).
[16] J.-Y. Bigot, M. T. Portella, R. W. Schönlein, and C. V. Shank, Phys. Rev. Lett. **67**, 636 (1991).
[17] D.-S. Kim, J. Shah, J. E. Cunningham, T. C. Damen, S. Schmitt-Rink, and W. Schäfer, Phys. Rev. Lett. **68**, 2838 (1992).
[18] A. Honold, L. Schultheis, J. Kuhl, and C. W. Tu, Phys. Rev. B **40**, 6442 (1989).
[19] R. Hellmann, M. Koch, J. Feldmann, S. T. Cundiff, E. O. Göbel, D. R. Yakovlev, A. Waag, and G. Landwehr, J. Cryst. Growth **138**, 791 (1994).
[20] H. P. Wagner, J. Lehmann, and B. Hahn, J. Lumin. **66&67**, 84 (1996).
[21] A. J. Fischer, D. S. Kim, J. Hays, W. Sham, J. J. Song, D. B. Eason, J. Ren, J. F. Schetzina, H. Luo, and J. K. Furdyna, Phys. Rev. B **50**, 17 643 (1994).
[22] L. Schultheis, A. Honold, J. Kuhn, J. Köhler, and C. W. Tu, Phys. Rev. B **34**, 9027 (1986).
[23] D. S. Kim, J. Shah, J. E. Cunningham, T. C. Damen, W. Schäfer, M. Hartmann, and S. Schmitt-Rink, Phys. Rev. Lett. **68**, 1006 (1992).
[24] A. J. Fischer, D. S. Kim, J. Hays, W. Shan, J. J. Song, D. B. Eason, J. Ren, J. F. Schetzina, H. Luo, J. K. Furdyna, Z. Q. Zhu, T. Yao, J. F. Kiem, and W. Schäfer, Phys. Rev. Lett. **73**, 2368 (1994).
[25] M. A. Haase, J. Qiu, J. M. DePuydt, and H. Cheng, Appl. Phys. Lett. **59**, 1272 (1991).
[26] T. Saiki, K. Takeuchi, and M. Kuwata-Gonokamie, Appl. Phys. Lett. **60**, 192 (1992).
[27] D. Weckendrup, M. Saschek, U. Neukirch, J. Gutowski, S. O. Ferreira, and H. Sitter, J. Appl. Phys. **77**, 4145 (1996).
[28] H. P. Wagner, J. Lehmann, and B. Hahn, Solid-State Electron. **40**, 745 (1996).
[29] T. Häupl, H. Nickolaus, F. Henneberger, and A. Schülzgen, Phys. Status Solidi B **194**, 219 (1996).
[30] U. Neukirch, D. Weckendrup, K. Wundke, and J. Gutowski, J. Opt. Soc. Am. B **13**, 1256 (1996).
[31] H. Nickolaus, F. Henneberger, and A. Schülzgen, J. Cryst. Growth **159**, 780 (1996).
[32] H. P. Wagner, A. Schätz, R. Meier, W. Langbein, and J. Hvam, following paper, Phys. Rev. B **56**, 1797 (1997).
[33] T. Kuroda, K. Inoue, R. Kuribayashi, F. Minami, A. Mysyrowicz, and I. Suemune, J. Lumin. **66&67**, 429 (1996).
[34] V. Kozlov, P. Kellar, A. V. Nurmikko, C.-C. Chu, D. C. Grillo, J. Han, C. G. Hua, and R. L. Gunshor, Phys. Rev. B **53**, 10 837 (1986).
[35] A. Knorr, T. Stroucken, A. Schulze, A. Girndt, and S. W. Koch, Phys. Status Solidi B **188**, 473 (1995).
[36] M. Hubner, J. Kuhl, J. Stroucken, A. Knorr, S. W. Koch, R. Hey, and K. Ploog, Phys. Rev. Lett. **76**, 4199 (1996).
[37] T. Reisinger, Ph.D. thesis, Universität Regensburg, Germany, 1996.
[38] H. Preis, T. Frey, T. Reisinger, and W. Gebhardt (unpublished).
[39] M. Wörz, E. Griebl, Th. Reisifnger, B. Flierl, D. Haserer, T. Semmler, T. Frey, and W. Gebhardt, Phys. Status Solidi B **202**, 805 (1997).
[40] H. Mathieu, P. Lefebvre, and P. Christol, Phys. Rev. B **46**, 4092 (1992).
[41] H. P. Wagner, W. Langbein, and J. M. Hvam (unpublished).
[42] S. Jorda, U. Rössler, and D. Broido, Phys. Rev. B **48**, 1669 (1993).
[43] N. Miura, Y. Imanaka, and H. Nojiri, Mater. Sci. Forum **182–184**, 287 (1995).
[44] H. W. Hölscher, A. Nöhthe, and Ch. Uihlein, Phys. Rev. B **31**, 2379 (1985).
[45] S. Rudin, T. L. Reinecke, and B. Segall, Phys. Rev. B **42**, 11 218 (1990).